Geotechnical Engineering Journal of the SEAGS & AGSSEA Vol. 51 No. 2 June 2020 ISSN 0046-5828

FD Analysis on Piled Raft Foundation Settlements under Vertical Loads

D.W. Chang[1], H.W. Lien[2] and M.H. Hung[3]
[1,2,3]*Department of Civil Engineering, Tamkang University, New Taipei City, Taiwan*
[1]*E-mail*: dwchang@mail.tku.edu.tw

ABSTRACT: A three-dimensional finite difference analysis has been developed to estimate the foundation settlements for vertically loaded piled raft foundations. Thin-plate theory was adopted to model the finite raft with boundary effects. Alternate spring models were used to model soil resistances under the raft while the resistances of pile were model by calculating the pile stiffness from wave equation analysis. The newly proposed analysis was examined with finite element solutions. It was found that variations of soil resistance underneath the raft and the pile-soil-pile interactions are the keys to the applicability of such analysis.

KEYWORDS: Geocell reinforcement, Composite model, Flexible pavements, Parametric study

1. INTRODUCTION

Design and analysis of the piled raft foundation has been studied extensively since 1980s. The design guideline for combined pile raft foundation (CPRF) with the performance based design principles can be found in Katzenbach and Choudhury (2013). In general, capacities and deformations of the foundation are of design interest. As to the settlements of a combined pile raft foundation (CPRF), two-dimensional (2D) and/or three-dimensional (3D) analyses are both available. For 2D analysis, the raft can be treated as a one-dimensional (1D) beam on soil and pile-soil springs. Figure 1 illustrates the beam model of rigid and flexible rafts on clays. Notice that the complexities arise even for 2D analysis when choosing the soil springs *(*i.e., linear or nonlinear, clay or sand, etc.). The beam model namely the beam on elastic foundation or Winkler foundation is applicable when the length-to-width ratio (L/W) of the raft (where L is the length, W is the width) exceeds 10. The 2D analysis has been discussed for decades (Biot 1937; Mathews 1958, Bowles 1977, Ting and Mockry 1984, Jones 1997, Chen 1998, Tomlinson and Boorman 2001, Dinev 2012, Chiou et al. 2016, Chang et al. 2016). The shortcoming of such analysis is that the 3D geometry and load variations of the foundation can't be simulated closely.

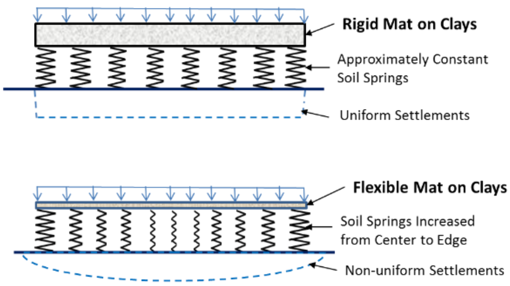

Figure 1 1D Beam model on a set of soil springs for rigid and flexible foundations

Alternatively, 3D analysis is modeled taking the raft as a two-dimensional plate (or mat) underlain by the soils and piles. Analytical formulations have been presented (Timoshenko and Krieger 1959, Vlasov and Leontev 1966, Kukreti and Ko 1992). Owing to complexities of the solutions, the analytical analyses are rarely used in engineering practice. Instead, numerical solution comprised a series of connecting strip footings can be found in Poulos (1991), a modified analysis was further suggested by Poulos (1994) for plate on soil continuums with boundary integrals. In general, the 3D analysis has been extensively studied in the past (Randolph 1983; Clancy and Randolph 1996, Horikoshi and Randolph 1996, Yamashita et al. 1998, Kitiyodom and Matsumoto 2002, Kitiyodom et al. 2005, Kobayashi et al. 2009). Figure 2 shows the typical model of the 3D simulations from Clancy and Randolph (1996). It should be noted that the raft-soil-raft interactions and the pile-soil-raft interactions can be captured by modeling closely the continuity of the raft with the soil springs and pile-soil elements attached to the raft. The pile-soil-raft interactions can be approximated if both pile-soil elements and soil springs were considered at the same positions where piles located. Such interaction can be trivial since the soils underneath the raft would only affect the soils at relatively shallow depths along the pile.

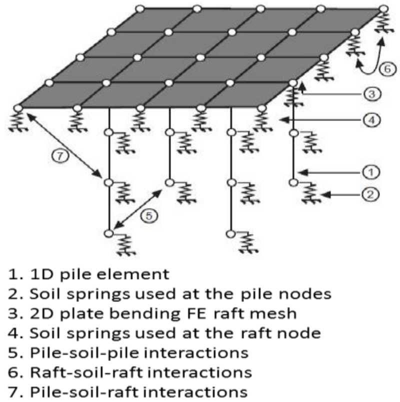

Figure 2 Piled raft foundation model with 2D raft (from Clancy and Randolph, 1996)

The 3D analysis for settlements of a CPRF can be conducted using either Equations of Motion formed by matrices of the structural elements or Wave Equations derived from the equilibriums of the whole structural system. The former solves the foundation settlements with stiffness matrix of the foundation (and the mass/damping matrices for dynamic problems) while the latter is often proceeded using difference formulas at the grids. For example, the raft can be modeled using either finite elements or simplified grid (beam-column) elements underlain by a set of applicable soil springs and pile-soil elements. With such modeling, the former solution would be resulted in. If the latter is adopted, one must derive the governing differential equation of the structural system, i.e., the wave equation. The corresponding finite difference solution of the wave equation of a 2D plate (as the raft) can be found in Bowles (1977). Such analysis is only applicable to an infinite raft or a rigid raft where the foundation settlements are nearly uniform. For a flexible raft where the differential settlements are important, the solution suggested by Bowles (1977) needs modifications. As to the CPRF, the soils and pile-soil elements can be attached to the 2D raft in order to simulate the resistances underneath the foundation.

With such concern, this paper introduces a composed 3D finite difference analysis for a CPRF foundation at the ground surface subjected to vertically uniform static load. The governing differential equation from the Thin Plate theory was first modified with the boundary values where the moments and shears were vanished. The equivalent stiffness of the pile-soil element was able to compute using the one-dimensional wave equation derived on the pile-soil segments. Afterwards, such equivalent pile stiffness was adopted together with the soil springs to support the raft foundation. The proposed analysis was then verified with three-dimensional FEM analysis to ensure its application.

2. MODEELING THE RAFT

Theory of Plate can be categorized as thin plate and thick plate. In general if the thickness of the plate (D) is less than a tenth of the width (W) of plate, it can be treated as thin-plate. The Kirchhoff-Love classical plate theory was suggested for thin plate. The Thick Plate theory considers the in-plane shear strains whereas the Thin Plate theory does not.

2.1 Governing Equation

According to Timoshenko and Woinowsky-Krieger (1959), governing equation of the vertical displacements of a thin plate subjected to vertically uniform load (q) and point load (P) can be written as follows,

$$\frac{\partial^4 w}{\partial x^4} + \frac{2\,\partial^4 w}{\partial x^2\,\partial y^2} + \frac{\partial^4 w}{\partial y^4} = \frac{12q(1-\nu^2)}{ED^3} + \frac{12P(1-\nu^2)}{ED^3(\partial x\,\partial y)} \quad (1)$$

where w is the vertical displacement of the raft, ν and E are the Poisson's ratio and Young's modulus of raft, D is thickness of the raft, and *x* and *y* are the spatial variables. Bowles (1977) has demonstrated the finite difference formula of the above equation for the infinite plate. It should be noted that the soil resistances underneath the raft need to be considered if such analysis was adopted.

2.2 Boundary Conditions

For a raft foundation located at the ground surface as shown in Figure 3, the moments and shear forces are assumed zero at edge of the foundation. The top and bottom edges of the raft where *y*=constant, Mx (bending moment rotating at the *x*-direction) and Vy (vertical shear force at the surface normal to *y*-direction) can be written as follows,

$$M_x = -B(\partial^2 w/\partial y^2 + \nu\,\partial^2 w/\partial x^2) = 0 \quad (2)$$

$$V_y = -B\left[\frac{\partial^3 w}{\partial y^3} + \frac{(2-\nu)\,\partial^3 w}{\partial y\,\partial x^2}\right] = 0 \quad (3)$$

where B is the expression of $ED^3/(12(1-\nu^2))$. Similarly, at the left and right edges of the raft where *x*=constant, the boundary conditions M_y and V_x are:

$$M_y = -B(\partial^2 w/\partial x^2 + \nu\,\partial^2 w/\partial y^2) = 0 \quad (4)$$

$$V_x = -B\left[\frac{\partial^3 w}{\partial x^3} + \frac{(2-\nu)\,\partial^3 w}{\partial x\,\partial y^2}\right] = 0 \quad (5)$$

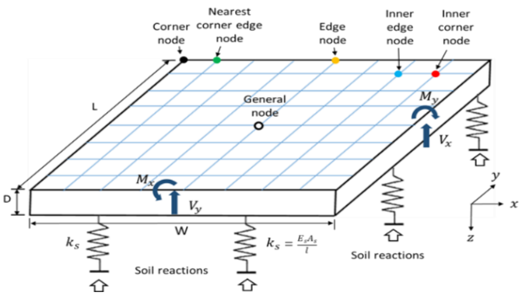

Figure 3 2D model of the raft on ground surface (from Chang *et al.* 2018)

Eqs. (2)~(5) can be incorporated with Eq. (1) to derived for the finite difference formulas on the settlements of a finite-dimensions raft under vertical loads. Figure 4 illustrates the nodal points used to derive the required formulations. As a result, there are six categories of the equations need to be solved. With the variations of nodal positions in the raft, there will be 25 types of the equations involved in the solutions. Details of the formulations can be found in Chang et al. (2018) and Lien (2018). For a square raft, if the length and width of the raft were both discretized by *m* nodes, then there will be m^2 nodes and m^2 equations developed in the raft. The solutions require to conduct the matrix analysis, in which the size of the augment matrix will be $m^2 \times m^2$. Computer program WERAFT-S was suggested for such modeling.

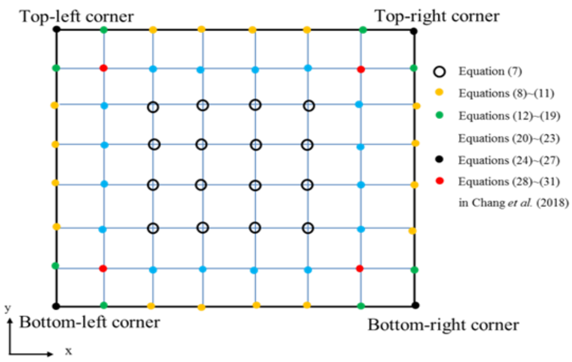

Figure 4 Allocations of the formulas used at the nodes of raft (from Chang *et al.* 2018)

2.3 Soil Resistances

For the soil resistance underneath the raft, various spring models can be used. For simplicity, the study considers the linear ones. For example, the rod stiffness and Lysmer's Analog model can be adopted. If rod stiffness was used, soil spring constant k_s can be computed as E_sA_s/l where E_s is the Young's Modulus of the soil, A_s is the effective area of the soils underneath the raft, and *l* is the length of the soil spring. Assuming that the underneath soil reactions are similar to the uniform pressures of the superstructure loads, Eq. (1) can be modified by replacing q with q^* where $q^* = q - \Sigma k_s w_k/A_r = q - (E_s/l)\,\Sigma A_{sk} \times w_k / A_r$; w_k is foundation settlement at the k^{th} node, A_{sk} is the area of the soil spring under the k^{th} node, and A_r is the total area of the raft which is equal to ΣA_{rk} where A_{rk} stands for the area of raft at the k^{th} node. Now defining q_k^* as the modified load allocated at the k^{th} node, q_k^* can be approximated by $q-(E_s/l)w_k(A_{sk}/A_{rk})$, where (A_{sk}/A_{rk}) is called as the area ratio (n) at the k^{th} node. Figure 5 illustrates the area ratios used at different nodal points inside and along the edge of the raft.

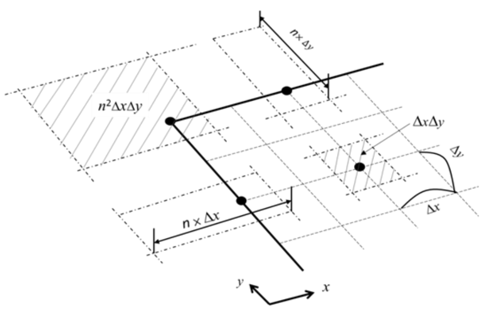

Figure 5 Effective area of the soils at nodes along the edge

Using the above simulations, Chang et al. (2018) has reported that the optimal length of the soil springs is approximately 20m for elastic soil layer with shear wave velocity (V_s) of 150m/s and Poisson's ratio (ν_s) of 0.4, whereas the optimal area ratio (n) for nodes along the edge of the raft is 2.5. Thus the optimal area ratio for the corner nodes would be 2.5×2.5=6.25.

For smaller raft which behaves more rigidly, the Lysmer's Analog spring model (Lysmer and Richart 1966) initially proposed for rigid foundation could be used. Note that the total soil spring constant Ks for soils underneath the raft was suggested as $4G_s r_o/(1-\nu_s)$, where G_s is the shear modulus of the soil, ν_s is the Poisson's ratio of the soil, and r_o is the equivalent radius of the raft foundation. If such soil spring model was adopted, the averaged spring constant, ks (i.e., ks=Ks/m^2) was used each node. The influence of the area ratio is neglected in this case. It should be noted that the actual soil resistances underneath a flexible foundation will not be uniform. Such phenomenon will be discussed later in this paper.

3. MODELING THE PILES

3.1 Governing Equation

For piles underneath the raft, equivalent stiffness of the piles (kp) was able to compute assuming linearly elastic soil springs attached to the piles (See Figure 6).

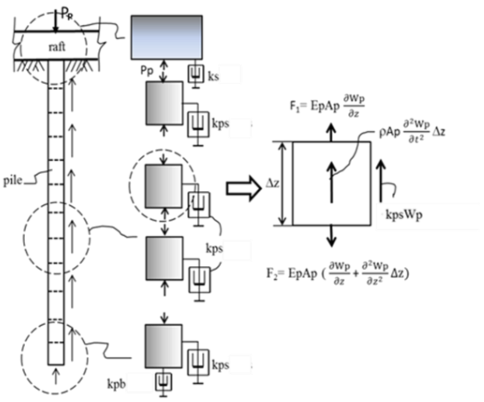

Figure 6 Pile-soil elements layout for discrete wave equation

The stiffness of the single piles can be analyzed assuming a unit load acting on the pile head. The governing differential equation of the pile segments upon the force equilibriums can be established as follows,

$$\mathrm{EpAp}\frac{\partial^2 \mathrm{wp}}{\partial z^2}dz = -\mathrm{kps} \times \mathrm{wp} \quad (6)$$

where Ep and Ap are the Young's modulus and area of the cross section of the pile, respectively. Wp is the displacement of the pile, and kps is stiffness of the soil springs attached to the pile.

3.2 Boundary Conditions

The force equilibriums at the pile head and the pile tip were suggested as follows,

$$\mathrm{EpAp}\frac{\partial \mathrm{wp}}{\partial z} = -\mathrm{Pp} \quad \text{at the pile head} \quad (7)$$

$$\mathrm{EpAp}\frac{\partial \mathrm{wp}}{\partial z} = -\mathrm{kpb}\times\mathrm{wp} \quad \text{at the pile tip} \quad (8)$$

where Pp is the load applied at the pile head, and kpb is the soil stiffness at the pile tip. Expressing Eq. (6) for the pile segments and eliminating the fictitious nodes with Eqs. (7)~(8), the discrete FD solutions for displacements of the pile segments under the vertical load can be obtained. The well-known computer program APILE (Reese 1987) is based on such modeling. Chang and Lin (1999) had successfully demonstrated the pile-to-pile interaction effects on grouped piles using such modeling.

3.3 Application of Pile-Soil Elements

For linear elastic pile behaviors, the equivalent stiffness (kp) of a single pile with surrounding soils can be easily obtained dividing the load by the displacement appearing at the pile head. Again for simplicity, the rod stiffness model can be used for the soil springs surrounding the pile. Thus the soil stiffness can be written by G_sA_s/l_s and E_sA_b/l_b for soils at shaft and pile tip, respectively. The parameters A_s and l_s are the corresponding area and the length of soil springs along the shaft where $A_s=\pi\times d$ (d is the pile diameter); parameters A_b and l_b are the corresponding area and the length of soil springs at pile tip, where $A_b=\pi d^2/4$. The equivalent pile stiffness, kp was examined with other soil models. By assuming that l_s and l_b are respectively 1m, the equivalent stiffness of the pile-soil element (kp) was found very similar to other models (See Table 1). The pile-soil elements can be combined with the soil springs to model the resistances under the raft. Therefore, Eq. (1) at the nodes where the pile locates without the column load P can be rewritten as follows,

$$\frac{\partial^4 \mathrm{w}}{\partial \mathrm{x}^4} + \frac{2\,\partial^4 \mathrm{w}}{\partial \mathrm{x}^2\,\partial \mathrm{y}^2} + \frac{\partial^4 \mathrm{w}}{\partial \mathrm{y}^4} = \frac{12\mathrm{q}''(1-\nu^2)}{\mathrm{ED}^3} \quad (9)$$

where q" is expressed as q" = q- (ks+kp)×w_k/A_r. Thus, the CPRF settlements can be calculated using the modified load intensity, q". Computer program WEAPR-S was suggested for CPRF settlement analysis under the statically uniform loads.

Table 1 Comparison of Pile Stiffness from Various Models

Model	K_s along shaft	K_b at bottom	Kp (kN/m)
Rod stiffness	$K_s = \frac{G_s A}{l_s}$ (l_s=1m)	$K_b = \frac{E_s A}{l_b}$ (l_h=1m)	130680
Liang (1993)	$K_s = \frac{2\pi L_i G_s}{\ln(2.5L_i(1-\mu_s)/r_0)}$	$K_b = \frac{\pi r_0 E}{2(1-\mu_s^2)I_b}$	144840
Matsumoto (2013)	$K_P = \frac{2\pi G\Delta L}{\ln(r_m/r_0)}$		131208

4. FOUNDATION SETTLEMENTS

The proposed analyses WERAFT-S and WEAPR-S were examined and compared with the solutions obtained from 3D FEM analysis using Midas-GTS NX (Midas, 2017). The numerical model of the CPRF and the soil layer as well as the corresponding material properties are shown in Table 2. The effects of the influence factors in the modeling are discussed next.

Table 2 Numerical Model Parameters and Dimensions in Use

Soils	Shear wave velocity (V_s) = 150m/s, ν_s=0.4, γ_s = 19 kN/m^3
Foundation	Concrete raft : 26m×26m×1m Concrete piles : round pile w/ diameter at 1m and length at 30m E=3×10^{4}Mpa, γ=24kN/m^3, ν=0.15
Load	Uniform load q with intensity of 100 kPa

4.1 WERAFT-S Analysis

In modeling the raft foundation settlements under the loads, the authors found that the results obtained by using the rod model springs are mainly varying with the compressibility of the soils (i.e., shear wave velocity and Poisson's ratio of the soils) and they are dependent of the optimal length (*l*) of the soil spring and the optimal area ratio (n). Figure 7 indicates the comparisons of WERAFT-S and FEM solutions on standard numerical model by varying the parameters of n and *l* independently. It seemed that when *l*=20m and n=2.5, the foundation settlements obtained from WERAFT-S were more agreeable with the FEM analysis.

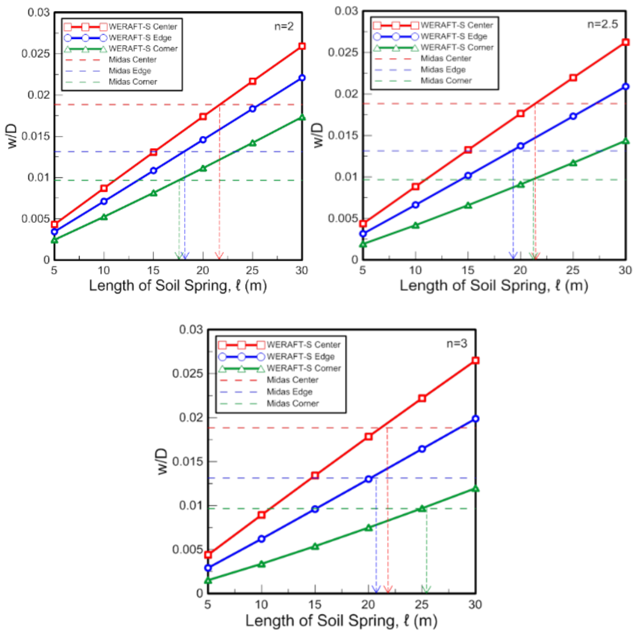

Figure 7 The influences of area ratio and length of soil spring on the rod stiffness model (from Chang *et al.* 2018)

Figures 8~9 depict the comparisons by changing the parameters V_s and ν_s of the soils. It can be found that the foundation settlements were varied at different locations following the order of $w_{center}>w_{edge}>w_{corner}$. Although the rod stiffness seems not adequate to be applied owing to the required length of the soil spring, the variations of the optimal length of the soil springs and the area ratio implies that the soil springs used in a flexible foundation should be varied at different locations.

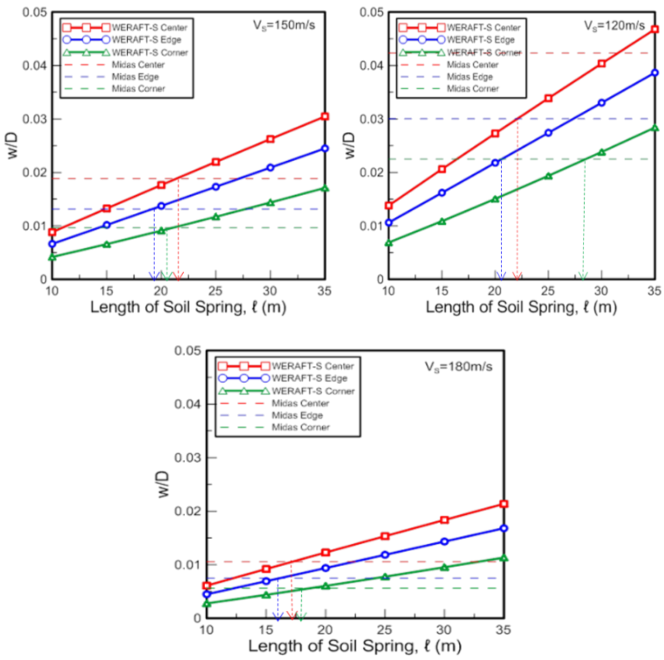

Figure 8 The influences of shear wave velocity of soil and length of soil spring on the rod stiffness model (from Chang *et al.* 2018)

The results of using Lysmer's Analog model as the soil springs are shown in Table 3. It should be noted that the settlements are comparable with the FEM solutions in the center and the middle edge of the raft when V_s=150m/s, however at the corner of the raft, the settlement obtained from WERAFT-S was found much smaller than

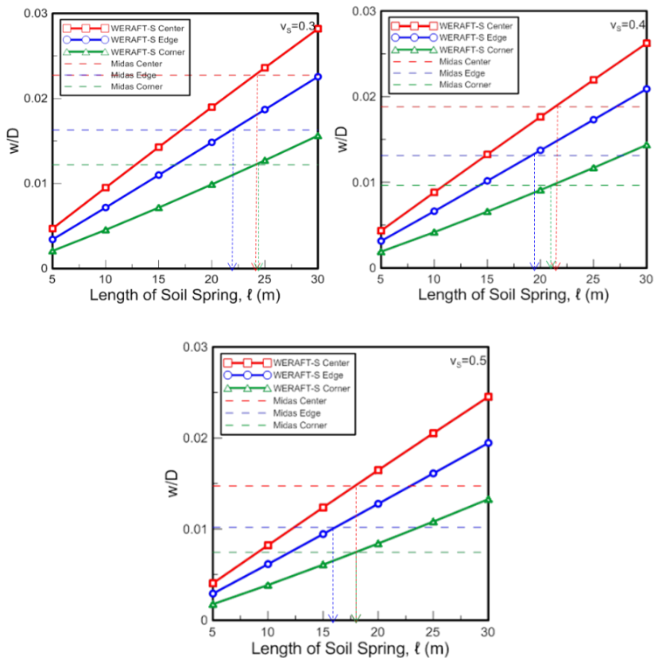

Figure 9 The influences of Poisson's ratio of soil and length of soil spring on the rod stiffness model (from Chang *et al.* 2018)

FEM calculated one. Moreover, large deviations of the results were found in the cases where V_s= 120m/s and V_s=180m/s. The values shown in Table 3 for V_s= 120m/s and 180m/s were obtained multiplying the foundation stiffness by a factor of 0.7 and 1.2, respectively. The deviations are believed to be caused by the Lysmer's model which was originally proposed for rigid foundation on elastic half-space while the FEM analysis was conducted for flexible foundation in a finite think soil layer.

Table 3 Foundation Settlements of the Raft

Shear wave velocity, V_s	Analysis	Midas-GTS	WERAFT-S w/ rod spring	WERAFT-S w/ Lysmer's spring
	Location	Settlement (mm)		
120 m/s	Center	42.3	40.3	40.4
	Edge	30.0	31.8	31.3
	Corner	22.5	22.7	20.0
150 m/s	Center	18.8	18.6	18.6
	Edge	13.1	13.7	13.6
	Corner	9.7	9.2	7.9
180 m/s	Center	10.6	11.1	10.8
	Edge	7.5	7.9	7.6
	Corner	5.6	5.1	4.2

4.2 WEAPR-S Analysis

In comparing the CPRF settlements from WEAPR-S (with the use of Lysmer's Analog springs) analysis with those from the FEM analysis, the foundation settlements calculated at the center and the middle edge were found similar for different analyses when S/d is equal to 8. Again, the ones found at the corners from the proposed analysis were found approximately half of those calculated from the FEM analysis. (See Figure 10 and Table 4) The differences appearing at the settlements of the corner were also found when the ground stiffness parameters (Vs and ν_s) were changed (see Figure 11). In addition, it was learnt that the pile-soil-pile interactions are significant when S/d became less than 8. The foundation settlements due to the changes of pile length were reproduced well except at the corners. (see Figure 12). Ignoring the pile-soil-pile interactions, the foundation settlements estimated by WEAPR-S were found much smaller than those obtained from the FEM analysis. Figure 13 shows the estimations obtained from WEAPR-S with the blind-guess reduction coefficient (β) to reduce the equivalent stiffness of the piles (kp) for the possible influences of the pile-soil-pile interactions. It can be seen that the rough reductions of equivalent pile stiffness due to the pile-soil-pile interactions can improve the results for CPRF with 7×7 and 5×5 piles.

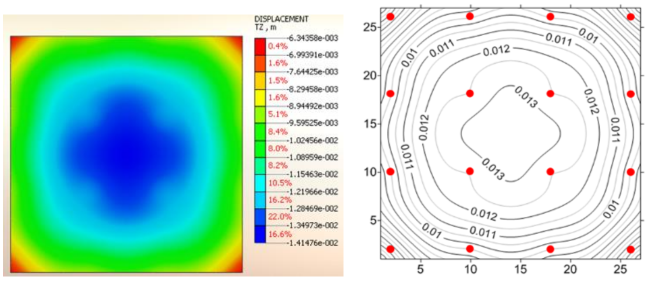

Figure 10 Contour plots for piled raft foundation settlements from WEAPR-S and FEM analysis, upper rom Midas-GTS analysis, bottom from WEAPR-S analysis with Lysmer's springs

Table 4 Foundation Settlements from WEAPR-S and FEM Analyses

Location	Midas-GTS NX	WEAPR-S	Deviation
Center	14.1mm	13.3mm	5.7%
Edge	9.6mm	9.4mm	2.1%
Corner	6.4mm	3.2mm	50%

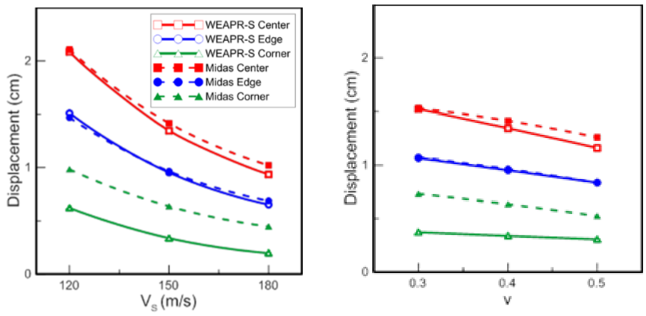

Figure 11 Comparisons on piled raft foundation settlements by varying V_s and v_s of soils

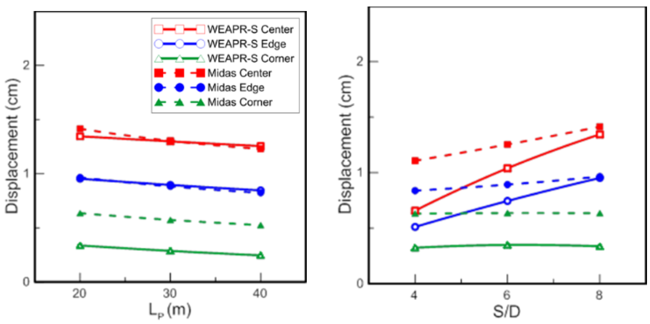

Figure 12 Comparisons on piled raft foundation settlements by varying length and S/d of the piles

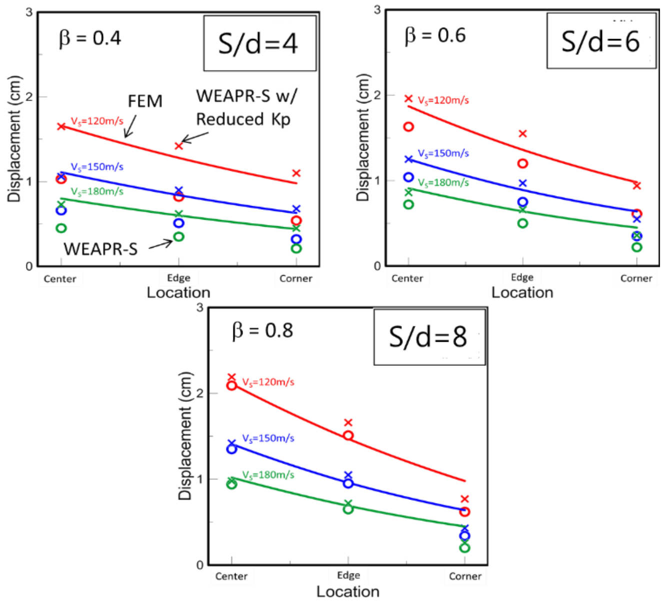

Figure 13 Comparisons of piled raft foundation settlements with and without reducing the equivalent stiffness of piles from WEAPR-S and FEM analyses

5. MODELING PROSPECTIVES

5.1 Feasible Soil Spring Model for Flexible Raft

To modify the soil spring model used for flexible foundation, the authors have conducted a study based on 3D FEM analysis. The variations of the soil resistances underneath the same numerical model can be interpreted with a normalized function $f(x)$ from the center to the right edge of the foundation, when y=0; and a normalized function $g(y)$ from the center to the top edge of the foundation, when x=0 (see Figure 14).

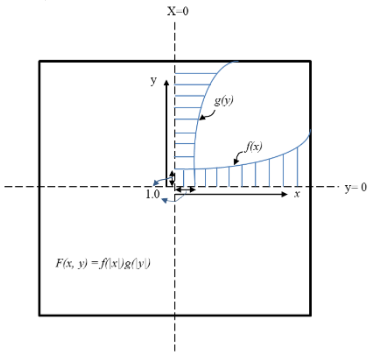

Figure 14 Schematic layout of the normalized functions for soil stiffness underneath the raft

Therefore two-dimensional normalized function $F(x,y)$ can be written as $f(|x|) \times g(|y|)$. Applying $F(x,y)$ to modify k_s (where $k_s=\{4G_s r_o/(1-\nu_s)\}/m^2$) for Lysmer's Analog spring, *i.e.*, $k_s^*=k_s \times F(x,y)$ with the finite depth influence (where H=60m) as shown in Eq. (10), the results obtained for WERAFT-S were studied and it was found that the discrepancies would be resulted at the foundation edge. Therefore, modification of the soil spring stiffness along the foundation edge is required. It was found that the soil spring constants need to be reduced to yield compatible displacements with the FEM ones. The reductions would be dependent of the soil stiffness. Detailed discussions on the modelling of the soil stiffness underneath a flexible raft can be found in Chang and Hung (2019). For the soils having shear wave velocity of 150 m/sec and Poisson's ratio of 0.4, the suggested equation of the normalized foundation stiffness can be found as follows,

$$f(x) = 2*10^{-7}x^6 - 7*10^{-17}x^5 - 2*10^{-5}x^4 - 4*10^{-13}x^3 + 0.0016x^2 + 10^{-10}x + 0.994 \quad (r^2=0.9998) \tag{9}$$

where x in above equation is the absolute value of the distance from the centre of the foundation.

5.2 Pile-Soil-Pile Interactions

To incorporate the pile-soil-pile interactions into the proposed analysis WEAPR-S, following procedures are suggested.

1. Compute CPRF settlements from WEAPR-S analysis with the equivalent pile stiffness. Initially the pile-soil-pile interactions can be excluded. Solve for the total loads carried by the piles, i.e., $Pp_{total} = \Sigma Pp_i$ where $Pp_i = kp_i \times wp_i$.
2. Compute the ratios of the displacements appeared at each pile head. For example, if a 3×3 piles were encountered (see Figure 15), the ratio of a (=wp_1/wp_2) and b (=wp_2/wp_5) can be computed, due to the symmetry of foundation settlements, wp_1/wp_2 must be equal to wp_3/wp_2, $wp_7/wp2$ and wp_9/wp_2. Similarly, wp_2/wp_5 must be equal to wp_4/wp_5, wp_6/wp_5 and wp_8/wp_5.
3. With the use of approximate pile-to-pile interaction factor α_v suggested by Dobry and Gazetas (1988) for grouped piles under statically vertical loads (where ω=0rps), the corresponding equations can be established to solve for the percentages of the loads carried at each pile (p_i). The required equations can be found in Chang *et al.* (2019)
4. Once the new loads carried by each pile ($Pp_i^* = Pp_{total} \times p_i$) were computed, the equivalent stiffness of each pile can be calculated again as $kp_i^* = Pp_i^*/wp_i$, replace kp_i by kp_i^*.
5. Repeat steps No.1 to No.5 to solve for wp_i and the corresponding p_i and kp_i^*. The analysis is iterated and stopped until the variations of both kp_i^* and/or wp_i are becoming trivial.

The above procedures are now studied by the authors (Chang, 2019) to learn the reductions of the equivalent stiffness of the piles taking into account of the influences of pile-soil-pile interactions.

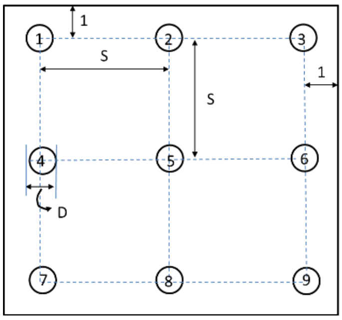

Figure 15 Plan view of a 3×3 piled raft foundation and its orientations

6. CONCLUDING REMARKS

This paper presents a newly proposed three-dimensional finite difference modeling for the foundation settlements of combined pile raft foundations (CPRF) under vertically uniform loads. Numerical model of a square CPRF was monitored with the boundary influences. The analysis was found to provide rational results in comparison with the 3D FEM analysis for foundation settlements at the center and the edge. The settlements at the corner were found much smaller than those suggested by the FEM analysis. The finite thickness of the soil layer used in the FEM analysis is deviated to the proposed analysis where the foundation was assumed resting on the surface of ground with infinite thickness. In addition, the soil stiffness should be varying underneath the raft while the foundation deformed more like a flexible one. The Lysmer's analog model used for the soil springs under rigid foundation will result in some deviations. The drawback of such modeling can be improved by using the rod stiffness for the soils with the enlarged areas at the edge. The estimations were found more agreeable for the foundation settlements. Normalized function for the soil resistance is then suggested for flexible raft. As to the settlements of combined pile raft foundation, the pile-to-pile interactions will become significant as the pile-to-pile spacing distance was reduced (*i.e.*, S/d<8). Such mechanism must be taken into account in the proposed analysis to yield accessible solutions.

7. ACKNOWLEDGEMENTS

The content of this paper is partial result of the research grant MOST-106-2211-E-032-025-MY2. The authors express sincere gratitude towards the funding.

8. REFERENCES

Biot, M.A., (1937). Bending of an infinite beam on an elastic foundation. Journal of Applied Physics, 12 155-164.

Bowles, J.E., (1977). Foundation Analysis and Design, 2nd ed., McGraw-Hill Companies, Inc.

Chang, D.W., (2019) Stiffness reduction of piles due to pile-to-pile interactions for piled raft foundation under vertical load, Research Grant, MOST-108-2221-E-032-007.

Chang, D.W., Lee, M.R., Hong, M.Y. and Wang, Y.C., (2016). A simplified modeling for seismic responses of rectangular foundation on piles subjected to horizontal earthquakes. J. of GeoEngineering, TGS, 11(3) 109-121.

Chang, D.W., Lien, H.W. and Wang, T.Y., (2018). Finite difference analysis of vertically loaded raft foundation based on the plate theory with boundary concern. J. of GeoEngineering, TGS, 13(3) 135-147.

Chang, D.W. and Hung, M.H., (2019). Modeling of Soil Stiffness of Flexible Foundations under Vertical Loads, *Research Report*, Dept. of Civil Engineering, Tamkang University. (under preparation)

Chang, D.W., Lien, H.W., Hu, G.Y, and Chuang, Y.A. (2019) "Developing a three dimensional finite-difference analysis for piled raft foundation settlements under vertical loads" *Procds*. The 4th International Conf. on Deep Foundations" Santa Cruz, Bolivia, May 22-23.

Chang, D.W. and Lin, K.C., (1999). Interaction effect on vertical pile response from time-domain wave equation analysis. Procds., The 2nd Int. Conf. on Earthquake Geotechnical Engineering, Lisbon, Portugal, June, Vol. 1, 407-412.

Chen, C.N., (1998). Solution of beam on elastic foundation by DQEM. Journal of Engineering Mechanics, ASCE, 124(12) 1381-1384.

Chiou, J.S., Lin, H.S., Yeh, F.Y., and Sung, Y.C., (2016). Plastic settlement evaluation of embedded railroads under repeated train loading. Journal of GeoEngineering, TGS, 11(2) 97-107.

Clancy, P. and Randolph, M.F., (1996). Simple design tools for piled raft foundations. Geotechnique, 46(2) 313-328.

Dinev, D., (2012). Analytical solution of beam on elastic Foundation by singularity functions. Engineering Mechanics, ASCE, 19(6) 381-392.

Dobry, R. and Gazetas, G. (1988). Simple method for dynamic stiffness a damping of floating pile groups, Geotechnique, 38 557-574.

Elsabee, F. and Morray, J.P., (1977). Dynamic Behavior of Embedded Foundations. Dept. of Civil Engr. MIT, report R77-33.

Horikoshi, K. and Randolph, M.F., (1996). Estimation of overall settlement of piled rafts. Soils and Foundations, JGS, 39(2) 59-68.

Jones, M., (1997), Analysis of Beams on Elastic Foundations: Using Finite Difference Theory, ICE pub.

Katzenbach, R. and Choudhury, D., (2013). ISSMGE Combined Pile-raft Foundation Guideline, Technische Universitat Darmstadt, Institute and Laboratory of Geotechnics, Darmstadt, Germany.

Kausel, E. and Ushijima, R. (1979). Vertical and Torsional Stiffness of Cylindrical Footings. Dept. of Civil Engr. MIT, report R79-6.

Kitiyodom, P. and Matsumoto, T., (2002). A simplified analysis method for piled raft and pile group foundations with batter piles. Int. Journal for Numerical and Analytical Methods in Geomechanics, 26 1349-1369.

Kitiyodom, P., Matsumoto, T. and Kawaguchi, K., (2005). A simplified analysis method for piled raft foundations subjected to ground movements induced by tunneling. Int. Journal for Numerical and Analytical Methods in Geomechanics, 29 1485-1507.

Kobayashi, H., Nishio, H., Nagao, T. Watanabe, T., Horikoshi, K., Matsumoto, T., (2009). Design and construction practices of piled raft foundations in Japan. Procds., Int. Conf. on Deep Foundations - CPRF and Energy Piles, 101-135.

Kukreti, A.R. and Ko, M.G., (1992). Analysis of rectangular plate resting on an elastic half space using an energy approach. Applied Mathematical Modeling, 16(7) 338-356.

Liang M., (1993). Simplified dynamic method for pile-driving control", Journal of Geotechnical Engineering, 119(4), 694-713.

Lien, H.W., (2018). Finite Difference Analysis of Piled Raft Foundations under Vertically Loads, Master Thesis, Dept. of Civil Engineering, Tamkang University, Taiwan (in Chinese).

Lysmer, J. and Richart, F.E. Jr., (1966). Dynamic responses of footings to vertical loading. J. of the Soil Mechanics and Foundation Division, ASCE 92 SM1 65-91.

Matsumoto, T., (2013). Personal communications - lecture notes on piled raft foundations.

Mathews, P.M., (1958). Vibrations of a beam on elastic foundation. Journal of Applied Mathematics and Mechanics, 38(3-4) 105-115.

Midas, (2017). Midas GTS NX User Manual, Midas IT Co.

Omer, J.R. and Arbabi, A., (2015). Evaluation of finite element, finite difference and elasticity methods for hypothetical raft foundations installed on layered strata. Geotechnical and Geological Engineering, 33(4) 1129-1140.

Poulos, H.G., (1991). Analysis of piled strip foundation. Computer Methods and Advances in Geomechanics, ed. Beer et al., Rotterdam, 1, 183-191.

Poulos, H.G., (1994). An approximate numerical analysis of pile-raft Interactions. Int. J. for Numerical and Analytical Methods in Geomechanics, 18 73-92.

Randolph, M.F., (1983). Design of Piled Foundations, Cambridge Univ. Eng. Dept., Res. Rep. Soils TR143.

Reese, L., (1987). APILE1 Program Manual, Ensoft, Inc. Austin, TX USA.

Timoshenko, S. and Woinowsky-Krieger, S., (1959). Theory of Plates and Shells, 2nd ed., McGraw-Hill. New York.

Ting, B.Y. and Mockry, E.F., (1984). Beam on elastic foundation finite element. Journal of Structural Engineering, ASCE, 110(10) 2324-2339.

Tomlnison, M.J. and Boorman, R., (2001). Foundation Design and Construction, 7th ed. Addison-Wesley Longman Ltd.

Vlasov, V.Z. and Leontev, U.N., (1966). Beams, Plates and Shells on Elastic Foundation. (Translated from Russian), Israel Program for Scientific Translation Jerusllem, Israel.

Yamashita, K., Yamada, T. and Makurai, M., (1998). Simplified method for analyzing piled raft foundations. Deep Foundations on Bored and Auger Piles, Van Impe and Haegeman (eds), Balkema, Rotterdam, 457-464.